The added value of spaceborne passive microwave soil moisture retrievals for forecasting rainfall-runoff partitioning

W. T. Crow
USDA Agricultural Research Service, Hydrology and Remote Sensing Laboratory, Beltsville, Maryland, USA

R. Bindlish
SSAI, Hydrology and Remote Sensing Laboratory, Beltsville, Maryland, USA

T. J. Jackson
USDA Agricultural Research Service, Hydrology and Remote Sensing Laboratory, Beltsville, Maryland, USA

Received 18 May 2005; revised 22 July 2005; accepted 18 August 2005; published 17 September 2005.

[1] Using existing data sets of spaceborne soil moisture retrievals, streamflow and precipitation for 26 basins in the United States Southern Great Plains, a 5-year analysis is performed to quantify the value of soil moisture retrievals derived from the Tropical Rainfall Measuring Mission (TRMM) Microwave Imager (TMI) X-band (10.7 GHz) radiometer for forecasting storm event-scale runoff ratios. The predictive ability of spaceborne soil moisture retrievals is objectively compared to that obtainable using only available rainfall observations and the antecedent precipitation index (*API*). The assimilation of spaceborne observations into an *API* soil moisture proxy is demonstrated to add skill to the forecasting of land surface response to precipitation. **Citation:** Crow, W. T., R. Bindlish, and T. J. Jackson (2005), The added value of spaceborne passive microwave soil moisture retrievals for forecasting rainfall-runoff partitioning, *Geophys. Res. Lett.*, *32*, L18401, doi:10.1029/2005GL023543.

1. Introduction

[2] Within small and intermediate-scale basins, knowledge of antecedent soil moisture conditions provides a key source of skill for short-term (1- to 3-day) streamflow forecasting. Current operational approaches in the United States attempt to exploit this skill by estimating soil moisture through consideration of antecedent precipitation indices and/or the application of surface water balance models. In the near future, supplemental surface soil moisture information will be operationally available from microwave remote sensing. Previous work examining the added value of observed soil moisture for streamflow forecasting have considered observations derived from spaceborne radar [*Pauwels et al.*, 2002; *Francois et al.*, 2003], airborne passive [*Goodrich et al.*, 1994; *Jacobs et al.*, 2003], and in situ sensors [*Aubert et al.*, 2003]. Less work has been focused on soil moisture data estimates derived from passive spaceborne radiometers. Utilizing passive spaceborne observations for surface soil moisture retrievals presents an unique set of advantages (e.g. more frequent and spatially extensive observations than spaceborne radar, airborne passive, or ground-based observations and generally higher accuracy than spaceborne radar) and disadvantages (e.g. relatively poor spatial resolution). Examining the effect of these attributes on streamflow forecasting is further motivated by the expected windfall of global, passive-based soil moisture data expected from the upcoming Soil Moisture and Ocean Salinity (SMOS) [*Kerr et al.*, 2001], Hydrosphere State (Hydros) [*Entekhabi et al.*, 2004] and Conically Scanning Microwave Imager/Sounder (CMIS) [*Chauhan*, 2003] spaceborne missions.

[3] A critical benchmark for evaluating the value of such observations for hydrologic forecasting is whether their inclusion into a modeling system leads to improvements above and beyond what is possible using existing observational resources. Within the context of rainfall-runoff modeling, the issue is whether remotely-sensed soil moisture provides information concerning antecedent soil moisture that is more valuable for hydrologic forecasting than soil moisture proxies that are commonly available from observations of antecedent precipitation and simple soil moisture modeling.

[4] Using long-term daily rainfall/runoff data sets collected as part of the MOdel Parameterization EXperiment (MOPEX), satellite-based precipitation observations from the Global Precipitation Climatology Project (GPCP), and nearly five years of remotely-sensed soil moisture derived from the 10.7-GHz band of the Tropical Rainfall Mission (TRMM) Microwave Image (TMI), this analysis examines the value of simple precipitation-based soil moisture proxies - derived with and without the assimilation of remotely-sensed soil moisture retrievals – for the short-term (1–3 day) forecasting of storm event-scale runoff ratios (runoff/precipitation). The goal will be to definitely isolate the added value (if any) of spaceborne soil moisture retrievals for forecasting land surface response to precipitation.

2. Data

[5] MOPEX data sets provide high-quality, daily observations of streamflow, air temperature, and precipitation for a large number of intermediate-scale (500 to 10000 km^2) basins in the United States [*Schaake et al.*, 2001]. Prior to their inclusion into MOPEX, individual basins are screened according to the quality (and density) of rain gauges observations in the basin and degree of anthropogenic

0094-8276/05/2005GL023543$05.00

Table 1. Outlet Location, Basin Size, and Long-Term Runoff Ratios for MOPEX Basins Used in the Analysis

Basin	USGS Number	Lat/Long	Size, km^2	Runoff Ratio
1	02486000	−90.178/32.281	7927	0.263
2	06908000	−93.196/38.992	2800	0.294
3	06913500	−95.256/38.616	3125	0.236
4	06933500	−91.977/37.929	7100	0.229
5	07019000	−90.591/38.505	9470	0.253
6	07052500	−93.461/36.805	2467	0.256
7	07056000	−92.745/35.983	2072	0.283
8	07057500	−92.248/36.622	1402	0.336
9	07058000	−92.304/36.626	1425	0.230
10	07067000	−91.014/36.991	4167	0.347
11	07068000	−90.847/36.621	5095	0.381
12	07144200	−97.387/37.832	3317	0.136
13	07144780	−97.935/37.844	1967	0.073
14	07147070	−97.012/37.795	1065	0.185
15	07147800	−96.994/37.224	4700	0.260
16	07152000	−97.277/36.811	4647	0.211
17	07172000	−96.315/37.003	1112	0.232
18	07177500	−95.954/36.278	2262	0.254
19	07183000	−95.430/37.890	9545	0.216
20	07186000	−94.566/37.245	2910	0.213
21	07196500	−94.920/35.921	2397	0.282
22	07197000	−94.838/35.921	767	0.270
23	07243500	−96.065/35.675	5045	0.195
24	07290000	−90.696/32.347	7030	0.340
25	07346000	−94.498/32.749	2125	0.244
26	08055500	−96.944/32.965	6147	0.103

diversion and impoundment. All MOPEX basins within a box extending from −99 to −90 degrees longitude and south of 39 degrees latitude (the maximum latitude of TRMM observations) are considered (Table 1). To the west of −99 degrees longitude, runoff magnitudes are generally too low (1 to 2% of annual rainfall) to obtain an adequate sample of storm events with significant streamflow responses, and the predominance of forested land cover east of −90 degrees latitude greatly complicates the remote retrieval of soil moisture.

[6] The retrieval of surface soil moisture observations from 10.7 GHz TMI observations is described in detail by *Bindlish et al.* [2003]. Retrievals have a −3dB spatial resolution of 38^2 km^2. Due to TRMM orbital characteristics, overpass times vary but retrievals are generally available on a daily basis. Satellite-based precipitation fields are derived from one latitude/longitude degree daily (1DD) Global Precipitation Climatology Project (GPCP) products based on infrared retrievals from the Television Infrared Observation Satellite (TIROS) Operational Vertical Sounder (TOVS) and the Geostationary Operational Environmental Satellite (GOES) and passive microwave measurements from the Special Sensor Microwave Imager (SSM/I) [*Huffman et al.*, 2001].

3. Soil Moisture Proxies

[7] Three different soil moisture proxies are calculated: the antecedent precipitation index (*API*), TMI-based surface soil moisture retrievals (θ_{TMI}), and *API* updated with daily θ_{TMI} using a Kalman filter (API_{TMI}). *API* for day i is defined as

$$API_i = \gamma API_{i-1} + P_i \tag{1}$$

where P_i is daily precipitation and γ is the loss coefficient. Both rain gauge data and satellite-based rainfall products will be used to estimate P.

[8] Kalman filtering is used to update *API* predictions from (1) with remotely-sensed surface soil moisture from TMI. The relationship between *API* and TMI-derived surface soil moisture (θ_{TMI}) is derived by fitting a linear least-squares regression line (with slope b and intercept a) to daily scatter plots of each quantity. Due to the known sensitivity of this relationship to vegetation amount, separate fits are individually derived for each basin listed in Table 1. Using this measurement operator, the state update equation for the Kalman filter becomes

$$API^+_{TMI_i} = API^-_{TMI_i} + K_i\left(\theta_{TMI_i} - a - b\,API^-_{TMI_i}\right) \tag{2}$$

where K is the Kalman gain

$$K_i = b\,T_i^- / \left(b^2\,T_i^- + R\right), \tag{3}$$

T the forecasting error in model *API* predictions, and R the error in θ_{TMI} retrievals. Between daily updates, the model state API_{TMI_i} is temporally updated using (1). Forecasting error T is propagated in time using

$$T_i^- = \gamma^2\,T_{i-1}^+ + Q \tag{4}$$

and then adjusted at measurement times via

$$T_i^+ = (1 - b\,K_i)T_i^-. \tag{5}$$

The filter requires that two error parameters, Q and R, be set equal to the variance of daily error in *API* calculations and θ_{TMI} retrievals, respectively. Based on validation results for θ_{TMI} in *Bindlish et al.* [2003] and the known sensitivity of R to vegetation amount, R is assumed to be $(2\%)^2$ volumetric for basins in the lightly vegetated western portion of the region (west of −97 degrees latitude), $(4\%)^2$ for heavily vegetated eastern portions of the basin (east of −92 degree latitude) and $(3\%)^2$ for basins located in between. Following *Dee* [1995], modeling error is calculated by tuning Q such that normalized filter innovations - $[\theta_{TMI_i} - (a + b\,API_{TMI_i}^-)]^2/(b^2T_i^- + R)$ - have a temporal mean of one. During tuning, all basins are lumped together to obtain a single calibrated Q value.

4. Approach

[9] For each of the 26 basins described in Table 1, *API*, θ_{TMI}, and API_{TMI} were calculated on a daily basis between December 1997 and September 2002. Each moisture proxy was then used to estimate moisture levels on the day prior to the start of a storm event. The value of various soil moisture proxies for runoff forecasting were intercompared based on the Spearman-rank correlation coefficient (S_R) calculated between their pre-storm value and the subsequent time-integrated runoff ratio (total streamflow/total rainfall) observed during the event.

[10] A storm event is initiated when at least 2 mm of rainfall is recorded on single day and lasts for the next 7 days or until a day of above-threshold rainfall is recorded

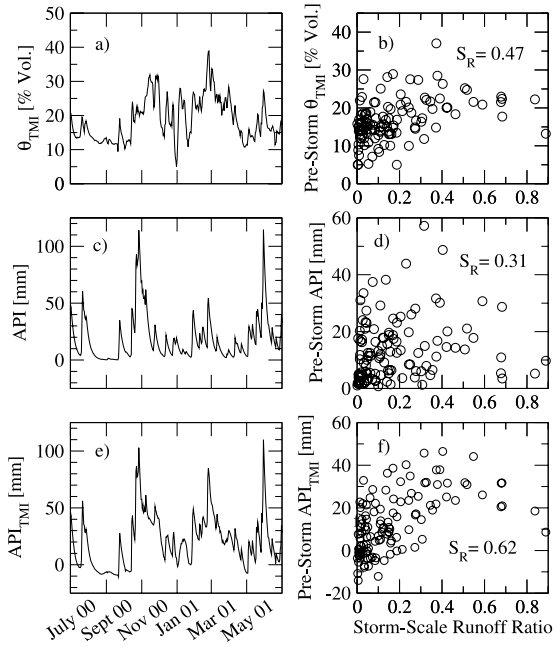

Figure 1. For a single basin (USGS number 07243500), 1-year time series of soil moisture proxies and scatter plots (for all five years) of proxies on the day prior to precipitation events versus subsequent storm event-scale runoff ratios. Each circle represents a separate event. Spearman-rank correlation coefficients (S_R) are given for each scatter plot.

following a day of below-threshold rainfall. To limit the impact of convoluted streamflow responses from closely following storms, only events lasting 5 days or more were considered and any event preceded by streamflow greater than 2 mm day^{-1} was deemed too close to a preceding event and dropped from the analysis. To minimize the impact of frozen precipitation, events beginning on days in which the average of minimum and maximum temperature was below 0 C were also masked. For the remaining events, cumulative rainfall and streamflow totals were obtained by summing observations made within individual storm periods and used to calculate a storm-scale runoff ratio (total streamflow/total precipitation) for each event. No attempt was made to separate out the base flow component of streamflow.

5. Results

[11] Figure 1 shows time series of θ_{TMI}, *API* and API_{TMI} proxies for a single basin (Deep Fork River at Beggs, OK - USGS number 07243500) between July 2000 and June 2001 and, for storms between December 1997 and September 2002, scatter-plots of pre-storm values of each proxy versus subsequent storm-scale runoff ratios. All three proxies demonstrate a positive and statistically significant Spearman-rank correlation coefficient (S_R) between their pre-storm values and subsequent storm-scale runoff ratios. A higher correlation coefficient is obtained for the merged API_{TMI} proxy (Figure 1f) than for either θ_{TMI} or *API* in isolation (Figures 1b and 1d). Figure 2a repeats the analysis for all 26 basins in Table 1 and plots S_R values calculated between the pre-storm value of proxies and subsequent event-scale runoff ratios. Despite exhibiting more basin-to-basin variability, S_R values for θ_{TMI} are generally comparable with correlation levels for *API*. However, the merger of θ_{TMI} into *API* to form API_{TMI} increases the observed correlation for all 26 basins (Figure 2a).

5.1. Impact of Satellite-Based Precipitation

[12] Only basins with sufficiently dense ground-based rain gauge observations are considered in MOPEX. Consequently the reliability of daily rainfall accumulations used to derive *API* values in Figures 1 and 2 is very high and not globally representative of typical rainfall accuracies. The results in Figure 2b are based on modifying the analysis in Figure 2a by using satellite-based GPCP-1DD daily rainfall estimates instead of rain gauge data to estimate P in (1). Switching between gauge- and satellite-based precipitation products leads to a reduction in the ability of *API* to forecast runoff-ratios (Figure 2b). However, when TMI observations are assimilated into *API*(GPCP) to form API_{TMI}(GPCP), the increase in S_R is large enough to fully compensate for the deficiencies of the GPCP-1DD precipitation forcing (Figure 2b). That is, an appropriate combination of satellite-based precipitation and *TMI* soil moisture observations provides as much (or more) land surface information than high quality rain gauge-based *API* predictions lacking any soil moisture assimilation.

5.2. Impact of Model Complexity

[13] *API* results for all basins in Figure 2 were derived assuming γ = 0.85 in (1). Sensitivity tests (not shown) reveal little qualitative variation in Figure 2 when γ is varied. However, given that (1) represents an extremely simplistic soil moisture model, it is worthwhile to consider the impact of increased model complexity. If daily temperature data is available, then γ can be modified to reflect

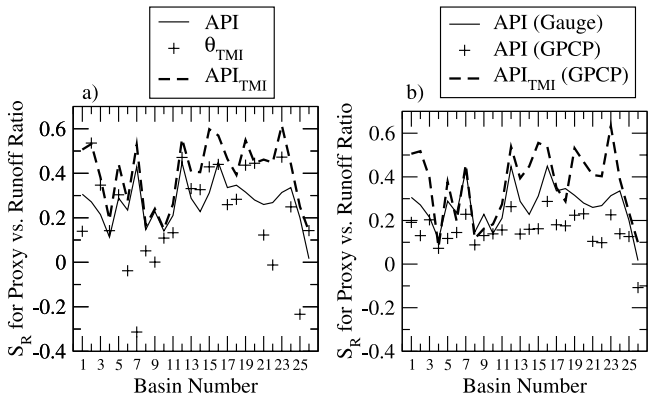

Figure 2. a) Comparison of S_R calculated between pre-storm values of soil moisture proxies versus storm event-scale runoff ratios using gauge-based precipitation and *API*, θ_{TMI}, and API_{TMI} proxies. Basin numbers on the x-axis correspond to the first column of Table 1. b) Same as a), except proxies are gauged-based *API* (*API*(Gauge)), satellite-based *API* (*API*(GPCP)), and the merged proxy based on the assimilation of θ_{TMI} into *API*(GPCP) (API_{TMI}(GPCP)).

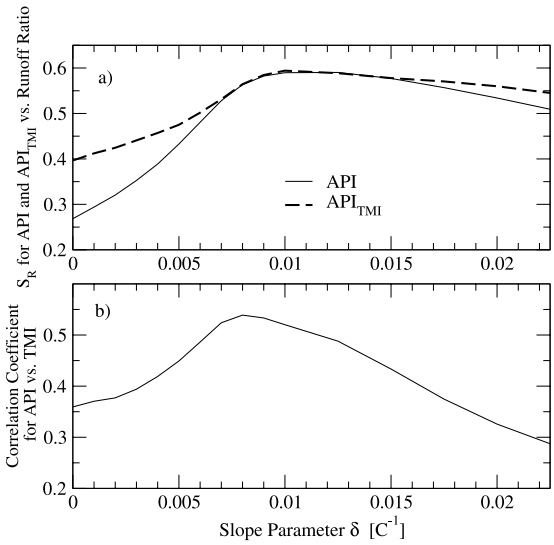

Figure 3. Impact of δ in (6) on a) the added value of assimilating θ_{TMI} into an *API* model and b) the Pearson's correlation coefficient observed between *API* and θ_{TMI}.

enhanced (reduced) soil loss due to evapotranspiration during warm (cold) days

$$\gamma = 0.85 + \delta(20 - T_{\max}[\mathrm{C}]) \quad (6)$$

where $T_{\max}$ is the daily maximum temperature and δ a sensitivity parameter. Figure 3a demonstrates how results change for this model modification by plotting S_R (averaged across all 26 basins) between event-scale runoff-ratio and both *API* and API_{TMI} for various choices of δ in (6). Gauge-based precipitation observations were used for all results and γ values bounded at a maximum value of one. Note that each choice for δ requires a separate recalibration of Q in (4) to maintain proper innovation statistics. A δ of zero corresponds to the previous approach where γ is fixed. At δ = 0, Figure 3a demonstrates that the assimilation proxy API_{TMI} is superior to just *API*. However, increasing δ leads to a sharper rise in S_R values for *API* than for API_{TMI}. In fact, near δ = 0.0075 [C^{-1}], the incremental value of assimilating θ_{TMI} into *API* vanishes. This suggests that for more complex models, the primary value of *TMI* observations will evolve towards the selection of static model parameters (i.e. calibration of δ) as opposed to the dynamic updating of *API* via data assimilation. Figure 3b illustrates the feasibility of this calibration strategy by demonstrating that values of δ associated with high S_R for *API* in Figure 3a are also associated with a high correlation between *API* and θ_{TMI}.

6. Summary and Conclusions

[14] Relative to the skill obtainable through consideration of only gauge-based antecedent precipitation, the assimilation of *TMI*-based soil moisture estimates (θ_{TMI}) into a simple *API* model leads to an enhanced ability to forecast rainfall-runoff partitioning (i.e. an increase in Spearman-rank correlation between pre-storm soil moisture proxies and subsequent storm-event runoff ratios) for all twenty-six of the basins listed in Table 1 (Figure 2a). The added value of *TMI* observations is enhanced when lower quality, but more readily available, satellite-based precipitation data sets are used to drive *API* predictions. In fact, Kalman filter-based assimilation of θ_{TMI} into an *API* model driven by satellite-based GPCP precipitation data leads to runoff-ratio forecasting skill that is slightly better than *API* models driven by high-quality ground-based gauge data (Figure 2b). That is, for this particular application, *TMI*-based soil moisture estimates are capable of compensating for the relative deficiency of satellite-based precipitation products versus higher-quality (but less readily available) rain gauge observations.

[15] However, the added value of assimilating θ_{TMI} is sharply reduced when an *API*-based approach is properly calibrated to exploit air temperature observations (Figure 3a) - suggesting that the proper interpretation of air temperature data can effectively reproduce the innovative dynamic information provided by the remotely-sensed soil moisture data. In such cases, the primary value of remote sensing observations will be for calibration of model parameters (Figure 3b). Therefore, for this particular application, data assimilation will likely be the appropriate approach only when the limited availability (or poor quality) of modeling forcing data necessitates a simplistic modeling approach. However, relative to the 10.7 GHz TMI observations utilized here, future spaceborne surface soil moisture missions (e.g. SMOS and Hydros) will be based on lower frequency observations capable of improved retrieval accuracy and deeper soil sampling volumes. These improvements will almost certainly enhance the value of remotely-sensed surface soil moisture products for hydrologic applications.

[16] **Acknowledgments.** The authors would like to thank the NOAA Office of Hydrology for providing access to MOPEX data sets. This research was partially supported by NASA EOS grant 03-0204-0265.

References

Aubert, D., C. Loumagne, and L. Oudin (2003), Sequential assimilation of soil moisture and streamflow data in a conceptual rainfall-runoff model, *J. Hydrol.*, *280*, 145–161.

Bindlish, R., T. J. Jackson, E. F. Wood, H. Gao, P. Starks, D. Bosch, and V. Lakshmi (2003), Soil moisture estimates from TRMM Microwave Imager Observations over the southern United States, *Remote Sens. Environ.*, *85*, 507–515.

Chauhan, N. (2003), NPOESS Conical Microwave Imager/Sounder: Issues and progress, *Proc. IEEE Geosci. Remote Sens. Symp.*, *1*, 373–377.

Dee, D. P. (1995), On-line estimation of error covariance parameters for atmospheric data assimilation, *Mon. Weather Rev.*, *123*, 1128–1145.

Entekhabi, D., et al. (2004), The Hydrosphere State (Hydros) mission concept: An Earth system pathfinder for global mapping of soil moisture and land freeze/thaw, *IEEE Trans. Geosci. Remote Sens.*, *42*, 2184–2195.

Francois, C., A. Quesney, and C. Ottle (2003), Sequential assimlation of ERS-1 SAR data into a coupled land surface-hydrological model using an extended Kalman filter, *J. Hydrometeorol.*, *4*(2), 473–487.

Goodrich, D. C., T. J. Schmugge, T. J. Jackson, C. L. Unkrich, T. O. Keefer, R. Parry, L. B. Bach, and S. A. Amer (1994), Runoff simulation sensitivity to remotely sensed initial soil water content, *Water Resour. Res.*, *30*(5), 1393–1405.

Huffman, G. J., R. F. Adler, M. M. Morrissey, D. T. Bolvin, S. Curtis, R. Joyce, B. McGavock, and J. Susskind (2001), Global precipitation at one-degree daily resolution from mulitisatellite observations, *J. Hydrometeorol.*, *2*, 36–50.

Jacobs, J. M., D. A. Meyers, and B. M. Whitfield (2003), Improved rainfall/runoff estimates using remotely sensed soil moisture, *J. Am. Water Resour. Assoc.*, *39*(2), 313–324.

Kerr, Y. H., P. Waldteufel, J.-P. Wigneron, J.-M. Martinuzzi, J. Font, and M. Berger (2001), Soil moisture retrieval from space: the soil moisture and ocean salinity mission (SMOS), *IEEE Trans. Geosci. Remote Sens.*, *39*(8), 1729–1735.

Pauwels, R. N., R. Hoeben, N. E. C. Verhoest, F. P. De Troch, and P. A. Troch (2002), Improvements of TOPLATS-based discharge predictions through assimilation of ERS-based remotely-sensed soil moisture values, *Hydrol. Processes*, *16*, 995–1013.

Schaake, J., Q. Duan, V. Koren, and A. Hall (2001), Toward improved parameter estimation of land surface hydrology models through the Model Parameter Estimation Experiment (MOPEX), *IAHS Publ.*, *270*, 91–97.

R. Bindlish, SSAI, Hydrology and Remote Sensing Laboratory, Beltsville, MD 20705, USA.

W. T. Crow and T. J. Jackson, USDA Agricultural Research Service, Hydrology and Remote Sensing Laboratory, Room 104, Building 007, BARC-W, Beltsville, MD 20705, USA. (wcrow@hydrolab.arsusda.gov)